Kinetics of Microtubule Catastrophe Assessed by Probabilistic Analysis

David J. Odde,* Lynne Cassimeris,‡ and Helen M. Buettner*
*Department of Chemical and Biochemical Engineering, Rutgers University, Piscataway, New Jersey 08855, and ‡Department of Molecular Biology, Lehigh University, Bethlehem, Pennsylvania 18015 USA

ABSTRACT Microtubules are cytoskeletal filaments whose self-assembly occurs by abrupt switching between states of roughly constant growth and shrinkage, a process known as dynamic instability. Understanding the mechanism of dynamic instability offers potential for controlling microtubule-dependent cellular processes such as nerve growth and mitosis. The growth to shrinkage transitions (catastrophes) and the reverse transitions (rescues) that characterize microtubule dynamic instability have been assumed to be random events with first-order kinetics. By direct observation of individual microtubules in vitro and probabilistic analysis of their distribution of growth times, we found that while the slower growing and biologically inactive (minus) ends obeyed first-order catastrophe kinetics, the faster growing and biologically active (plus) ends ends did not. The non-first-order kinetics at plus ends imply that growing microtubule plus ends have an effective frequency of catastrophe that depends on how long the microtubules have been growing. This frequency is low initially but then rises asymptotically to a limiting value. Our results also suggest that an additional parameter, beyond the four parameters typically used to describe dynamic instability, is needed to account for the observed behavior and that changing this parameter can significantly affect the distribution of microtubule lengths at steady state.

INTRODUCTION

Microtubule assembly is fundamental to a number of cellular processes. For example, some of the most effective drugs for treating cancer (e.g., taxol and vinblastine) are also known to specifically alter microtubule assembly dynamics, suggesting that microtubule assembly is central to the process of cell division (Alberts et al., 1994). In nerve growth, microtubule assembly plays a similarly important role: when growing axons are treated with microtubule depolymerizing drugs, the axons stop growing and retract (Yamada et al., 1970; Daniels, 1972; Bamburg et al., 1986). Therefore, understanding how microtubules assemble can lend valuable insight into important medical problems such as the treatment of cancer and the development of nerve regeneration strategies.

Microtubule assembly occurs by abrupt and apparently random switching between alternate phases of growth and shrinkage, a process called dynamic instability (Mitchison and Kirschner, 1984; Horio and Hotani, 1986; Cassimeris et al., 1988; Walker et al., 1988). These phases are persistent as thousands of tubulin subunits are added (or lost) in a single growth (or shrinkage) excursion. The growth to shrinkage transition (catastrophe) and the reverse transition (rescue) have been assumed to proceed with first-order kinetics, each with its own rate constant (Hill, 1984; Mitchison and Kirschner, 1987; Bayley et al., 1989; Verde et al., 1992; Dogterom and Leibler, 1993; Gliksman et al., 1993; Flyvbjerg et al., 1994). This assumption allows a simple and parsimonious description consistent with the stochastic nature of microtubule assembly. The first-order model carries an additional constraint, however. The model implies that a catastrophe (or rescue) is equally probable to occur at any instant during a growth phase and is not dependent on the past history of the system.

Alternatively, a microtubule may have built into its mechanism of assembly some form of dependence on its past which will influence its present and future behavior. This type of "memory" would manifest itself by non-first-order transition kinetics which can be identified from the distribution of phase times. If the transitions are first order, as has been assumed, then the distribution of phase times will be exponential (Olkin et al., 1980). Conversely, if the transitions are non-first-order, then the distribution of phase times will be nonexponential. To test whether microtubules have non-first-order catastrophe kinetics, we observed individual microtubules assembled from purified tubulin by video-enhanced differential interference contrast (VE-DIC) microscopy and obtained growth time distributions for both the plus and minus ends. While minus end growth times were well described by an exponential distribution, plus end growth times were not. An alternative model for the plus end distribution was identified and a new parameter describing microtubule assembly introduced. In addition, an existing molecular assembly model was examined for non-first-order kinetics and the potential physiological relevance of non-first-order kinetics demonstrated.

Received for publication 26 January 1995 and in final form 14 June 1995.

Address reprint requests to Dr. Helen M. Buettner, Department of Chemical and Biochemical Engineering, Rutgers University, P. O. Box 909, Piscataway, NJ 08855-0909. Tel.: 908-445-2231; Fax: 908-445-2421; E-mail: buettner@zodiac.rutgers.edu.

0006-3495/95/09/796/07 $2.00

MATERIALS AND METHODS

Tubulin and axoneme preparation

Porcine brain tubulin was purified by 2 cycles of assembly and disassembly, phosphocellulose chromatography, and a final assembly cycle in PEM buffer (0.1 M Pipes, 2 mM EGTA, 1 mM $MgSO_4$, 1 mM GTP, pH 6.9)

supplemented with 1 M glutamate (Walker et al., 1988). The tubulin pellet was resuspended in PEM buffer, clarified, and stored at −75°C. One tubulin preparation was used for all the experiments. No microtubule-associated proteins were detected by silver staining of overloaded SDS-PAGE (50 μg/lane; Walker et al., 1988). Tubulin concentrations were determined as previously described (Drechsel et al., 1992). Before each experiment, a small aliquot of tubulin was thawed, stored on ice, and used within 1–2 h. Axoneme fragments from *Strongylocentrotus. purpuratus* were purified as previously described (Walker et al., 1988) and stored at −20°C in 50% glycerol and washed in PEM buffer before use.

Microtubule assembly

Axoneme fragments were allowed to adhere to a glass coverslip in a humid chamber for 5 min. The coverslip was then sealed onto a glass slide along the top and bottom edges with Valap (1:1:1 Vaseline, lanolin, and paraffin) using parafilm pieces as spacers. This chamber was flushed with 80 μl of PEM buffer followed by perfusion of 80 μl of 6 μM tubulin in PEM buffer. The two remaining edges of the coverslip were than sealed with Valap and the assembly mounted on the microscope for imaging of individual, nucleated microtubules.

Videomicroscopy

The assembly of individual, axoneme-nucleated microtubules at 35°C was observed by VE-DIC microscopy (Schnapp, 1986; Salmon et al., 1989). A Nikon Microphot-SA equipped with 60×/1.4 NA DIC Plan Apo lens, DIC prisms and 1.4 NA condenser was used. Illumination was by a 100-W mercury lamp passed through an Ellis light scrambler (Technical Video, Woods Hole, MA). The microscope stand was also equipped with heat absorbing and 546-nm interference filters. Images were projected through a 5× projection lens to a Hamamatsu C-2400 newvicon video camera. Images were further enhanced using an Argus 10 (Hamamatsu) image processor for real-time, two-frame exponential averaging. The processed signal was passed through a time date generator (For-A Corp.) and recorded onto super VHS video tapes (Sony SV0–9500 MD). An air stream stage incubator (Nicholson Precision Instruments) was used to maintain a constant temperature of 35°C on the stage (a period of 5 min was allowed to permit chamber warmup). No sample was observed longer than 1 h.

Data analysis

Individual length life histories were obtained by digital image analysis of videotaped recordings (via RTM software courtesy of E. D. Salmon) and used to identify initiation and catastrophe events as shown in Fig. 1. Growth times were computed by taking the difference between the time of catastrophe (dark arrows) and the time of initiation (gray arrows), although on rare occasions microtubules initiated from rescue events (not shown). Some growth times at the beginning of a sequence were estimated by back-extrapolating to 0 length (gray line) since the growth rates were approximately constant and rescues were rare. All microtubules in a given field that could be tracked unambiguously were analyzed and no microtubules were observed to continuously grow over an entire observation period (maximum 50 min). Microtubules were classified as plus or minus based on their growth rate which was estimated by fitting a least-squares line (Walker et al., 1988).

Probability models

Exponential cumulative distribution functions of the form

$$F(t) = 1 - e^{-\theta t} \qquad (1)$$

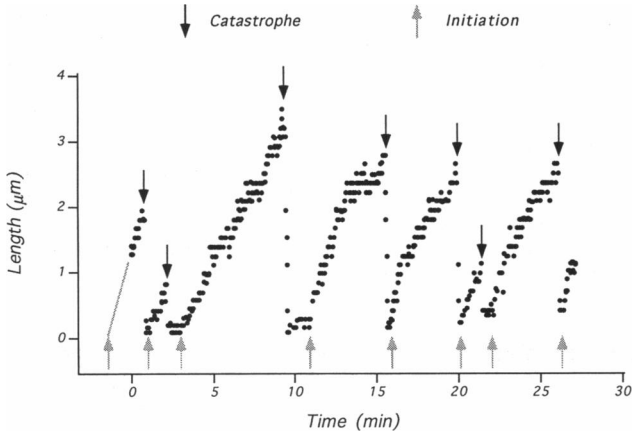

FIGURE 1 Microtubule length life history. The characteristic "saw-tooth" pattern of dynamic instability was exhibited by microtubules assembled from purified porcine brain tubulin (6 μM) using axoneme fragments as nucleating structures and observed by VE-DIC microscopy.

were fit to both the plus and minus end data by nonlinear least-squares minimization (Press et al., 1992). A gamma cumulative distribution function, given by

$$F(t) = \int_0^t \frac{\theta^r t^{r-1} e^{-\theta t}}{\Gamma(r)}\, dt \qquad (2)$$

with parameters r and θ, was fit to the plus end data by the same method.

Effective catastrophe frequency

An effective catastrophe frequency was defined as the rate at which microtubules undergo catastrophe, given that they have already been growing for a period of time. An effective catastrophe frequency defined in this way is a function of time and can be derived from the original cumulative distribution functions (Eqs. 1 and 2). First, a conditional cumulative distribution function was constructed to describe the distribution of times, y, beyond an arbitrary time, t^*, given that the microtubule has already grown for t^* (Olkin et al., 1980). The conditional cumulative distribution function is given by

$$G(y) = \frac{F(t^* + y) - F(t^*)}{1 - F(t^*)} \qquad y \geq 0 \qquad (3)$$

$$G(y) = 0 \qquad y < 0 \qquad (4)$$

where $F(u)$ is the appropriate cumulative distribution function (from either Eq. 1 or Eq. 2). The conditional cumulative distribution function, $G(y)$, was then differentiated with respect to y, evaluated at $y = 0$, and plotted as a function of t^*. This resulted in an effective catastrophe frequency at any instant in time t^*. For the exponential distribution this was simply equal to θ.

Lateral cap model simulations

A FORTRAN program was written to simulate dynamic instability with the lateral cap model as described by Bayley et al. (1990). Briefly, the model assumes 13 protofilaments in a 5-start helix with subunits in the lattice existing in either in a GTP or GDP state (Chen and Hill, 1985). Addition and loss of subunits occurs with rate constants that depend on the GTP/GDP state of neighboring subunits in the lattice. In the lateral cap model, hydrolysis is directly coupled to subunit addition so that the GTP cap is at

most one subunit layer deep. The basic parameter set described in Bayley et al. (1990) was used as well as the eight variations of the basic parameter set. All simulations were run at the critical concentration, which is the tubulin concentration at which no net growth occurs. For the basic parameter set this concentration was 5.9 μM, essentially the value used experimentally. A total of 10,000 growth times and 10,000 shrinkage times were obtained. The duration of a growth phase was defined as the time required to go from an all GTP tip state to an all GDP tip state. The duration of a shrinkage phase was defined as the time to reverse the states again. These times were found to be essentially the same as the duration of growth and shrinkage determined by examination of length life histories.

Length distributions using a two-state model

A FORTRAN program was written to simulate dynamic instability using a generalized two-state model as described previously (Odde and Buettner, 1995). The parameters of dynamic instability were specified: the growth and shrinkage rates (V_g and V_s) and the mean growth and shrinkage times (t_g and t_s; inverses of catastrophe and rescue frequencies, respectively). The gamma distribution shape parameters $r_g = r_s = r$ were then set (which also fixed the gamma distribution parameters θ_g and θ_s, since $t_g = r_g/\theta_g$ and $t_s = r_s/\theta_s$). Growth and shrinkage times were chosen at random from gamma distributions for each phase, and a length life history was generated with lengths recorded at 1-s intervals. In each simulation the first 5,000 lengths were ignored to allow the system to reach steady state after which the next 50,000 lengths were recorded. All simulations were performed on a Sun Sparc 10 workstation (Sun Microsystems, Inc.).

RESULTS AND DISCUSSION

Analysis of growth time distributions

The first-order model for the phase transitions of dynamic instability has been assumed in previous theoretical treatments because it is the simplest possible mechanism and underlies a large number of biochemical processes. To test whether this model is generally valid, microtubules were assembled in vitro from purified tubulin and individual growth times obtained through VE-DIC and digital image analysis. The dynamic parameters for the plus and minus ends are summarized in Table 1. The sets of growth times were plotted as cumulative distributions and the exponential distribution (Eq. 1) fit to the data as shown in Fig. 2. While the minus end growth times were consistent with an exponential distribution ($p = 0.74$), the plus end growth times were not ($p = 0.026$). Thus, under these conditions, the first-order model for catastrophe is valid for minus ends but not for plus ends.

Because the plus end growth times were fit poorly by the exponential distribution, the gamma distribution was considered as an alternative (Olkin et al., 1980). As shown in Fig. 3A, the gamma distribution (Eq. 2) provided a statistically probable fit to the plus end growth time distribution ($p = 0.54$). Other distributions, such as the Weibull distribution, provided reasonable fits as well (not shown); we chose the gamma distribution as a prototype nonexponential distribution since it lends itself to construction of a simple kinetic model for catastrophe (see below). The differences in shape between the best-fit exponential and gamma probability densities (Fig. 3 *B*) show that microtubules with gamma distributed growth times are less likely to have very short and very long growth times and more likely to have intermediate times compared to microtubules with exponentially distributed growth times. The exponential and gamma distributions each have corresponding kinetic models for catastrophe, as shown in Fig. 3 *C*. While the exponential distribution implies a single first-order transition, the gamma distribution implies a series of first-order transitions (Olkin et al., 1980). The number of serial first-order transitions is equal to the shape parameter r which is ~3 for the plus end data. Therefore, if the mechanism of catastrophe is the same as that upon which the gamma distribution is derived, then catastrophe would occur by a series of three

TABLE 1 Summary of microtubule assembly data

	Plus	Minus
Mean growth time ± SD (min)	1.91 ± 1.19	3.88 ± 2.92
Mean growth rate ± SD (μm/min)	1.04 ± 0.20	0.51 ± 0.17
Number of growth phases	59	98

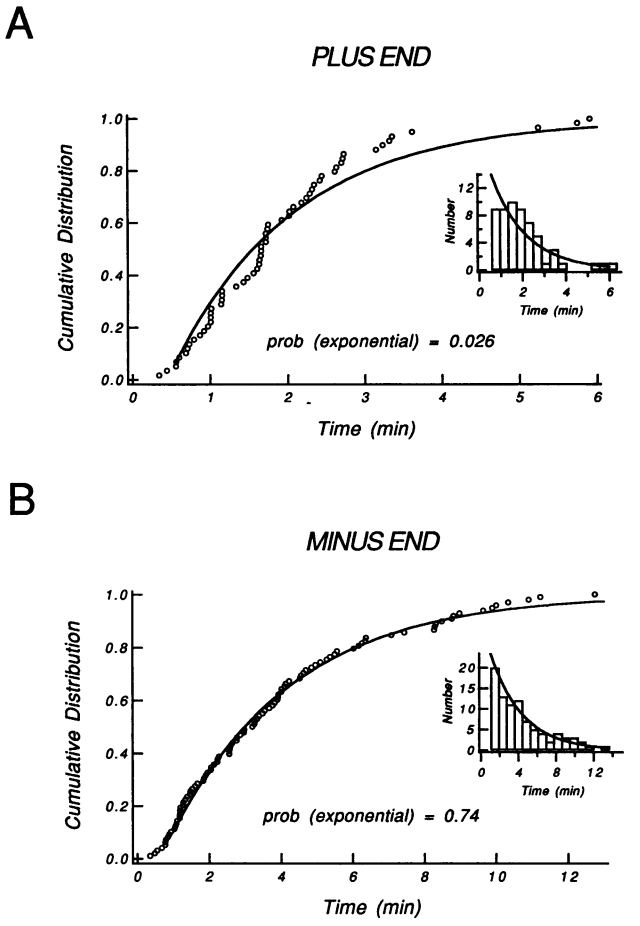

FIGURE 2 Plus and minus end growth time cumulative distributions. The open circles represent the experimentally measured growth times and the solid lines the best-fit exponential distribution. (*A*) Plus end data were not well described by an exponential distribution ($p = 0.026$). A histogram of the data, along with the fitted exponential model, is shown in the inset. (*B*) Minus end data were adequately described by the exponential distribution ($p = 0.74$).

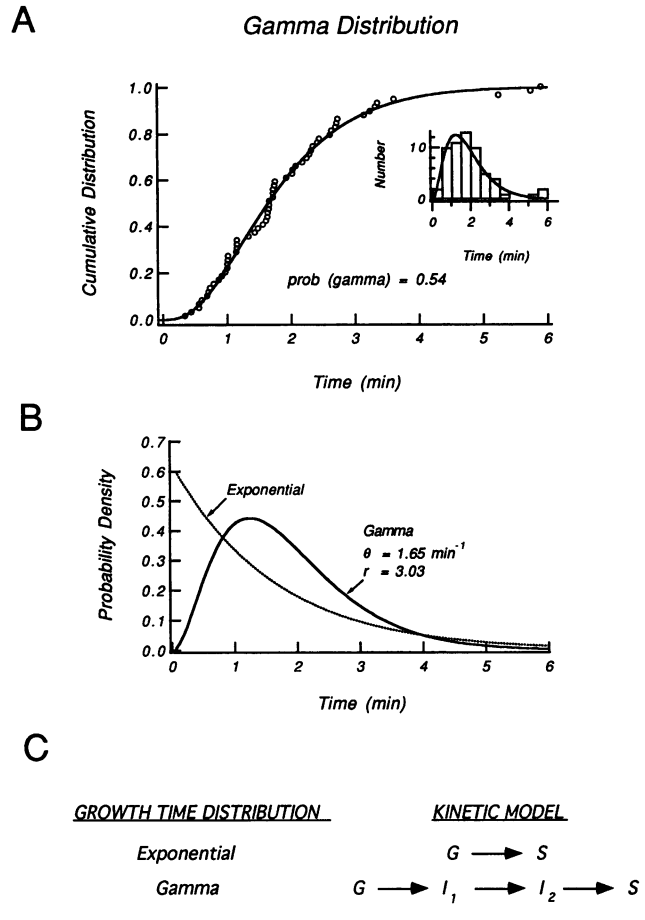

FIGURE 3 Gamma distribution fit to plus end data and implications for dynamic instability. (*A*) The gamma distribution (Eq. 2) adequately described the plus end growth time distribution (p = 0.54). (*B*) The best-fit gamma and exponential probability density functions using their best-fit parameter values from the plus end data. The gamma distributed growth times are "bunched" more in the middle range than the exponentially distributed growth times. (*C*) Probability distributions and their associated kinetic mechanisms.

first-order transitions each with rate constant θ (~1.7 min^{-1}). Each of these transitions could potentially represent key chemical or physical events occurring in the microtubule. Among these could be loss of a stabilizing GTP-tubulin cap at the microtubule tip (reviewed in Erickson and O'Brien, 1992) or induction of a structural change in the lattice (Mandelkow et al., 1991). Kinetic pathways other than the serial pathway shown in Fig. 3 *C* could probably account for the plus end distribution as well. In general, to obtain the sigmoidal shape of the cumulative distribution function (Fig. 3 *A*) these kinetic models will presumably require multiple events for catastrophe to occur.

Effective catastrophe frequency and microtubule memory

A microtubule that grows with first-order kinetics is equally likely to undergo catastrophe at any instant (Olkin et al., 1980). For this reason the frequency of catastrophe is independent of how long the microtubule has been growing as shown in Fig. 4. As a result, a microtubule with first-order kinetics has no sense of how long it has been growing and consequently lacks "memory" of its growth state. Alternatively, non-first-order catastrophe kinetics imply an effective catastrophe frequency that depends on how long the microtubules have been growing (Fig. 4). The effective catastrophe frequency is the instantaneous rate of catastrophe, given that a microtubule has already been growing for a period of time. For the gamma distribution fitted to the plus end data, microtubules have an effective catastrophe frequency near 0 at early times. Over time, the microtubules become more likely to undergo catastrophe, the effective catastrophe frequency asymptotically approaching a constant value at long times. The change in effective catastrophe frequency over time implies that the microtubules have a crude form of "memory" built into their mechanism of dynamic instability. This phenomenon can be visualized by imagining the progression of a microtubule through a series of states on the way to catastrophe (Fig. 3 *C*). Although each transition occurs randomly, catastrophe cannot occur until the microtubule has passed through each intermediate state. In this sense the microtubule can function as a nanometer-scale integrator of molecular events and perform a logical AND operation.

Kinetics of existing dynamic instability models

Dynamic instability is widely believed to be mediated by the acquisition and loss of a stabilizing cap of terminal GTP-tubulin subunits (Carlier and Pantaloni, 1981; Mitchison and Kirschner, 1984; O'Brien et al., 1987; Walker et al., 1988). Unfortunately, the presence of this putative cap has not been confirmed directly by experiment. An alternative

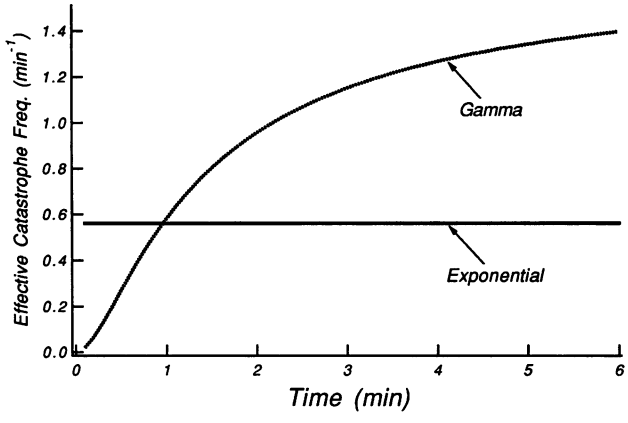

FIGURE 4 Effective catastrophe frequency for the exponential and gamma distribution growth time models. For the exponential distribution, the effective catastrophe frequency remains invariant over time and thus a growing microtubule has no "memory" of its growth state. Alternatively, for the gamma distribution, the effective frequency of catastrophe is initially low, rising asymptotically to a limiting constant value. In this sense, a growing microtubule has "memory" of its growth state since its effective catastrophe frequency depends on how long it has been growing.

approach has been to assume a mechanism for cap dynamics and simulate assembly using a computer (Chen and Hill, 1985; Bayley et al., 1990; Martin et al., 1993). The most viable of these computer models, the lateral cap model, assumes GTP hydrolysis is directly coupled to tubulin subunit addition (Bayley et al., 1990; Martin et al., 1993). Although somewhat speculative, this model can reproduce the two-state dynamics characteristic of dynamic instability (Bayley et al., 1990). Moreover, we find that the simulated growth and shrinkage times predicted by this model can be nonexponentially distributed as shown in Fig. 5. (the distributions shown here are for the basic parameter set but the other eight sets considered in the original description of the simulation model yielded similar distributions). The nonexponential nature of the distributions implies memory in both the catastrophe and rescue processes. It is difficult to assess the validity of the lateral cap model in any more detail because only a few of the eight model parameters can be measured directly from experiment. Even so, the lateral cap model, in contrast to simpler macroscopic models, is capable of producing nonexponentially distributed growth times.

The GTP cap model assumes that a microtubule is composed of an intrinsically labile lattice of GDP subunits stabilized by the GTP cap at the tip. If the cap is lost (through stochastic dissociation, for example), then the microtubule depolymerizes until restabilized by another GTP cap. Therefore, if one were to sever a microtubule in its midsection, the GTP cap hypothesis would predict immediate and extensive dissociation from the newly exposed ends of the microtubule until the tips are again stabilized by GTP caps. However, when microtubules are severed, either by an ultraviolet microbeam (Walker et al., 1989) or a glass needle (Tran and Salmon, 1993), the minus ends actually tend to grow while the plus ends rapidly dissociate as expected. Thus, the immediate growth behavior at minus ends apparently contradicts the GTP cap model. To explain these results, a three-state model of the form

$$G \Leftrightarrow I \Leftrightarrow S$$

has been proposed where G represents a growth state, S a shrinkage state, and I an intermediate state where the GTP cap is lost but the microtubule has not begun to disassemble (Tran and Salmon, 1993). A microtubule in this intermediate state can either recap (transit to state G) or start to disassemble (transit to state S). Except in cases where a particular transition is rate-limiting, the three-state model implies non-first-order catastrophe and rescue kinetics and hence memory in catastrophe and rescue. It is difficult to make direct comparisons between the cutting experiments and the present results since the cutting experiments presumably provide information about the rescue process while the present experiments provide information about catastrophe. Yet through these two diverse approaches the same conclusion has been reached: that catastrophe may require more than one event. In summary, the gamma distribution (two-state) model, the three-state model, and the lateral cap model, permit non-first-order catastrophe kinetics.

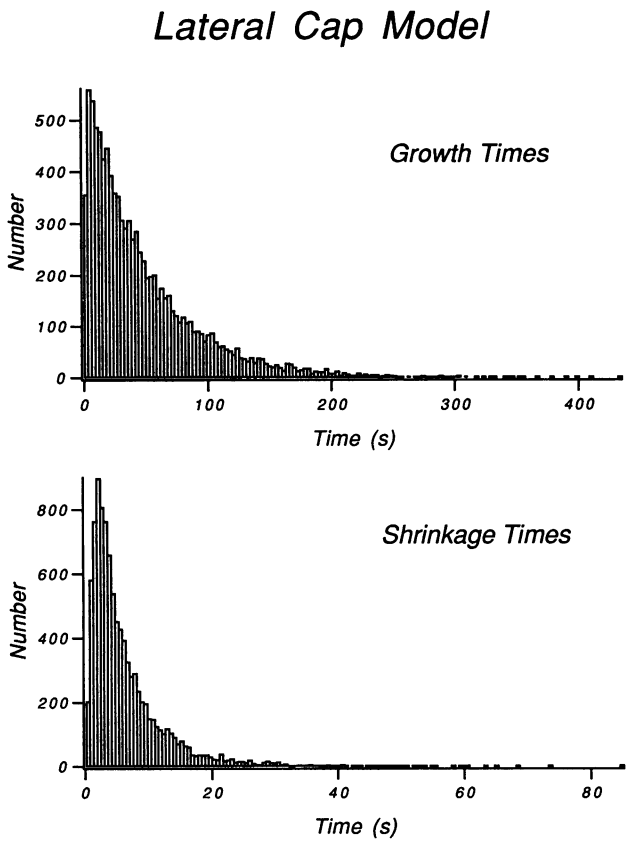

FIGURE 5 Growth and shrinkage time distributions for the lateral cap model. Both distributions are nonexponential implying non-first-order kinetics for both catastrophe and rescue. Eight other parameter sets yielded similar distributions (N = 10000).

Physiological relevance

The results presented here are for pure tubulin in vitro yet we expect that microtubules can exhibit non-first-order catastrophe kinetics in vivo as well based on the following evidence. First, despite the presence of stabilizing microtubule associated proteins (MAPs), individual microtubules have been observed to undergo dynamic instability in living cells (Cassimeris et al., 1988; Sammak and Borisy, 1988; Tanaka and Kirschner, 1991; Shelden and Wadsworth, 1993). Second, analysis of published microtubule assembly data from newt lung epithelia (Cassimeris et al., 1988) has suggested nonexponential growth and shrinkage time distributions (Odde and Buettner, 1995). Third, preliminary analysis of assembly data obtained for sea urchin extracts (Gliksman et al., 1992) has also suggested nonexponential behavior (not shown). In vivo, MAPs probably modulate the phase time distributions since they are known to modulate the parameters of dynamic instability in vitro (Drechsel et al., 1992; Pryer et al., 1992; Kowalski and Williams, 1993) and as such, modulation of distribution shape could be a means by which the cell regulates its distribution of microtubules.

To demonstrate the potential effect of phase time distribution shape on microtubule length distributions at steady state, we simulated nucleated microtubule assembly on a computer. Typically four parameters have been used in previous analyses to characterize dynamic instability (Hill, 1984; Mitchison and Kirschner, 1987; Bayley et al., 1989; Verde et al., 1992; Dogterom and Leibler, 1993; Gliksman et al., 1993; Flyvbjerg et al., 1994): the growth rate, V_g, the shrinkage rate, V_s, the catastrophe frequency, k_{cat} (inverse of mean growth time, t_g), and the rescue frequency k_{res} (inverse of mean shrinkage time, t_s). Modulation of these parameters has been shown to be a means by which the cell can regulate the assembly state of its microtubule array. In particular, modulation of the transition frequencies provides the means for cells to go from an interphase array, which is characterized by relatively long microtubules, to a mitotic array, which has an array of shorter microtubules (Belmont et al., 1990; Gliksman et al., 1993). In addition to the four parameters of dynamic instability we introduced two more parameters: a gamma distribution shape parameter for the growth time distribution, r_g, and a gamma distribution shape parameter for the shrinkage time distribution, r_s (Eq. 2). These parameters reflect the relative broadness of the phase time distribution with small r implying a broad distribution ($r = 1$ implies an exponential) and large r implying a narrower distribution (Fig. 3 *B*). As shown in Fig. 6 *A*, microtubules simulated with $r_g = r_s = r = 1$ have exponential length distributions at steady state as has been shown analytically (Hill, 1987). However, when the shape parameters are increased while holding the usual four parameters of dynamic instability (V_g, V_s, k_{cat}, and k_{res}) constant, the length distributions change (Fig. 6, *B,C*). These microtubules have a shorter mean length, and consequently more rapid turnover, characteristic of mitotic microtubule arrays. From the simulation results it can be seen that modulation of phase time distribution shape alone is capable of effecting the shortening in microtubule length observed in the transition from interphase to mitosis. Furthermore, the observed distribution of microtubule lengths in cultured human monocytes is nonexponential (Cassimeris et al., 1986), indicating that the simple first-order model ($r = 1$) by itself cannot adequately model dynamic instability. Thus we propose that a fifth dynamic instability parameter, r_g, characterizing the growth time distribution shape, and possibly a sixth parameter, r_s, (although we have not examined shrinkage time distributions) characterizing the shrinkage time distribution shape, are needed for a complete description of two-state microtubule assembly dynamics.

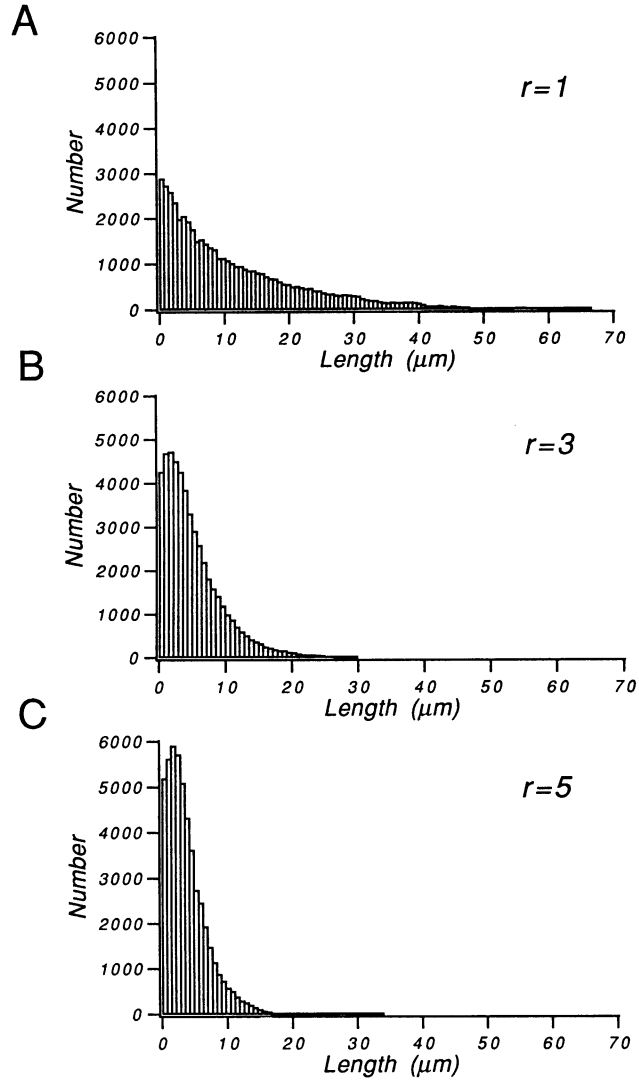

FIGURE 6 Microtubule length distribution at steady state and the effect of phase time distribution shape. The shape of the gamma distribution is determined by the parameter r, with increasing r indicating an increasingly narrow distribution of times (note: $r = 1$ is the exponential distribution). Steady-state length distributions are shown for (*A*) $r = 1$, (*B*) $r = 3$, and (*C*) $r = 5$ ($N = 50{,}000$). All other parameters being equal ($V_g = 14.5$ μm/min, $V_s = 17$ μm/min, $t_g = 17.9$ s, $t_s = 22.7$ s; see Fig. 6 in Gliksman et al., 1993), microtubules have longer average lengths when the phase time distributions are broad (i.e., exponential). The decreasing average length with increasing r is characteristic of an interphase-like to a mitotic-like transition in microtubule length distribution.

The distribution of growth times has implications for the proposed exploratory function of microtubules, where microtubules probe the cytoplasm by dynamic instability and then stabilize into preferred morphologies (Kirschner and Mitchison, 1986). In support of this hypothesis we find that microtubules exhibit a strong similarity in dynamic behavior to a known exploratory structure, the filopodium of nerve growth cones. Filopodia are thin, actin-based protrusions which extend from the growth cone periphery. They mediate signals from the extracellular environment, and thereby guide growth cones (Bentley and Toroian-Raymond, 1986). These linear structures extend out at a roughly constant rate for a random period of time and then rapidly transit to a retraction state if not stabilized by some positive interaction with the extracellular environment. Furthermore, quantitative analysis of chick growth cone filopodia in vitro suggests that the extension times are nonexponentially distributed (Buettner et al., 1994) with gamma distribution shape parameter r similar to the value we obtained for microtubule plus end growth times. Gamma distributed growth times would be well suited for exploration compared

to exponentially distributed growth times since less energy (e.g., in the form of GTP hydrolysis for microtubule assembly) is spent in extremely short and extremely long excursions (Fig. 3 *B*). Thus, the gamma distribution may represent a useful model for describing random, exploratory behaviors in complex systems.

Theoretical work was supported by a grant from the National Science Foundation to H.M.B. (BCS 92–10540) and experimental work by grants from the National Science Foundation to H.M.B. (IBN 94–09184) and L.C. (IBN 94–21046). The authors thank Dr. Neal Gliksman for sharing microtubule assembly data and Julius Fernandez for technical assistance with the lateral cap simulations. Julius Fernandez was supported by an REU Supplement to NSF BCS 92–10540.

REFERENCES

Alberts, B., D. Bray, J. Lewis, M. Raff, K. Roberts, and J. D. Watson. 1994. Molecular Biology of the Cell. 3rd ed. Garland Publishing, New York.

Bamburg, J. R., D. Bray, and K. Chapman. 1986. Assembly of microtubules at the tip of growing axons. *Nature.* 321:788–790.

Bayley, P. M., M. J. Schilstra, and S. R. Martin. 1989. A simple formulation of microtubule dynamics: quantitative implications of the dynamic instability of microtubule populations in vivo and in vitro. *J. Cell Sci.* 93:241–254.

Bayley, P. M., M. J. Schilstra, and S. R. Martin. 1990. Microtubule dynamic instability: numerical simulation of microtubule transition properties using a lateral cap model. *J. Cell Sci.* 95:33–48.

Belmont, L. D., A. A. Hyman, K. E. Swain, and T. J. Mitchison. 1990. Real-time visualization of cell cycle-dependent changes in microtubule dynamics in cytoplasmic extracts. *Cell.* 62:579–589.

Bentley, D., and A. Toroian-Raymond. 1986. Disoriented pathfinding by pioneer neurone growth cones deprived of filopodia by cytochalasin treatment. *Nature.* 323:712–715.

Buettner, H. M., R. N. Pittman, and J. K. Ivins. 1994. A model of neurite extension across regions of nonpermissive substrate: simulations based on experimental measurement of growth cone motility and filopodial dynamics. *Dev. Biol.* 163:407–422.

Carlier, M.-F., and D. Pantaloni. 1981. Kinetic analysis of guanosine 5′-triphosphate hydrolysis associated with tubulin polymerization. *Biochemistry.* 20:1918–1924.

Cassimeris, L., N. K. Pryer, and E. D. Salmon. 1988. Real-time observations of microtubule dynamic instability in living cells. *J. Cell Biol.* 107:2223–2231.

Cassimeris, L., P. Wadsworth, and E. D. Salmon. 1986. Dynamics of microtubule depolymerization in monocytes. *J. Cell Biol.* 102: 2023–2032.

Chen, Y., and T. L. Hill. 1985. Monte Carlo study of the GTP cap in a five-start helix model of a microtubule. *Proc. Natl. Acad. Sci. USA.* 82:1131–1135.

Daniels, M. P. 1972. Colchicine inhibition of nerve fiber formation in vitro. *J. Cell Biol.* 53:164–176.

Dogterom, M., and S. Leibler. 1993. Physical aspects of the growth and regulation of microtubule structures. *Phys. Rev. Lett.* 70:1347–1350.

Drechsel, D. N., A. A. Hyman, M. H. Cobb, and M. W. Kirschner. 1992. Modulation of the dynamic instability of tubulin assembly by the microtubule-associated protein tau. *Mol. Biol. Cell.* 3:1141–1154.

Erickson, H. P., and E. T. O'Brien. 1992. Microtubule dynamic instability and GTP hydrolysis. *Annu. Rev. Biophys. Biomol. Struct.* 21:145–166.

Flyvbjerg, H., T. E. Holy and S. Leibler. 1994. Stochastic dynamics of microtubules: a model for caps and catastrophes. *Phys. Rev. Lett.* 73: 2372–2375.

Gliksman, N. R., S. F. Parsons, and E. D. Salmon. 1992. Okadaic acid induces interphase to mitotic-like microtubule dynamic instability by inactivating rescue. *J. Cell Biol.* 119:1271–1276.

Gliksman, N. R., R. V. Skibbens, and E. D. Salmon. 1993. How the transition frequencies of microtubule dynamic instability (nucleation, catastrophe, and rescue) regulate microtubule dynamics in interphase and mitosis: analysis using a Monte Carlo computer simulation. *Mol. Biol. Cell.* 4:1035–1050.

Hill, T. L. 1984. Introductory analysis of the GTP-cap phase-change kinetics at the end of a microtubule. *Proc. Natl. Acad. Sci. USA.* 81:6728–6732.

Hill, T. L. 1987. Linear Aggregation Theory in Cell Biology. Springer-Verlag, New York.

Horio, T., and H. Hotani. 1986. Visualization of the dynamic instability of individual microtubules. *Nature.* 321:605–607.

Kirschner, M., and T. Mitchison. 1986. Beyond self-assembly: from microtubules to morphogenesis. *Cell.* 45:329–342.

Kowalski, R. J., and R. C. Williams Jr. 1993. Microtubule-associated protein 2 alters the dynamic properties of microtubule assembly and disassembly. *J. Biol. Chem.* 268:9847–9855.

Mandelkow, E.-M., E. Mandelkow, and R. A. Milligan. 1991. Microtubule dynamics and microtubule caps: a time-resolved cryo-electron microscopy study. *J. Cell Biol.* 114:977–991.

Martin, S. R., M. J. Schilstra, and P. M. Bayley. 1993. Dynamic instability of microtubules: Monte Carlo simulation and application to different types of microtubule lattice. *Biophys. J.* 65:578–596.

Mitchison, T. J., and M. W. Kirschner. 1984. Dynamic instability of microtubule growth. *Nature.* 312:237–242.

Mitchison, T. J., and M. W. Kirschner. 1987. Some thoughts on the partitioning of tubulin between monomer and polymer under conditions of dynamic instability. *Cell Biophys.* 11:35–55.

O'Brien, E. T., W. A. Voter, and H. P. Erickson. 1987. GTP hydrolysis during microtubule assembly. *Biochemistry.* 26:4148–4156.

Odde, D. J., and H. M. Buettner. 1995. Time series characterization of simulated microtubule dynamics in the nerve growth cone. *Ann. Biomed. Eng.* 23:268–286.

Olkin, I., L. J. Gleser, and C. Derman. 1980. Probability Models and Applications. Macmillan Publishing Co., Inc., New York.

Press, W. H., S. A. Teukolsky, W. T. Vetterling, and B. P. Flannery. 1992. Numerical Recipes in Fortran. 2nd ed. Press Syndicate of the University of Cambridge, New York.

Pryer, N. K., R. A. Walker, V. P. Skeen, B. D. Bourns, M. F. Soboeiro, and E. D. Salmon. 1992. Brain microtubule-associated proteins modulate microtubule dynamic instability in vitro. *J. Cell Sci.* 103:965–976.

Salmon, T., R. A. Walker, and N. K. Pryer. 1989. Video-enhanced differential interference contrast light microscopy. *BioTechniques.* 7:624–633.

Sammak, P. J., and G. G. Borisy. 1988. Direct observation of microtubule dynamics in living cells. *Nature.* 332:724–726.

Schnapp, B. J. 1986. Viewing single microtubules by video light microscopy. *Methods Enzymol.* 134:561–573.

Shelden, E., and P. Wadsworth. 1993. Observation and quantification of individual microtubule behavior in vivo: microtubule dynamics are cell-type specific. *J. Cell Biol.* 120:935–945.

Tanaka, E. M., and M. W. Kirschner. 1991. Microtubule behavior in the growth cones of living neurons during axon elongation. *J. Cell Biol.* 115:345–363.

Tran, P. T., and E. D. Salmon. 1993. Microtubule dynamic instability is a three-state process. *Mol. Biol. Cell.* 4:165a.

Verde, F., M. Dogterom, E. Stelzer, E. Karsenti, and S. Leibler. 1992. Control of microtubule dynamics and length by cyclin A- and cyclin B-dependent kinases in *Xenopus* egg extracts. *J. Cell Biol.* 118: 1097–1108.

Walker, R. A., S. Inoue and E. D. Salmon. 1989. Asymmetric behavior of severed microtubule ends after ultraviolet-microbeam irradiation of individual microtubules in vitro. *J. Cell Biol.* 108:931–937.

Walker, R. A., E. T. O'Brien, N. K. Pryer, M. F. Soboeiro, W. A. Voter, H. P. Erickson, and E. D. Salmon. 1988. Dynamic instability of individual microtubules analyzed by video light microscopy: rate constants and transition frequencies. *J. Cell Biol.* 107:1437–1448.

Yamada, K. M., B. S. Spooner, and N. K. Wessells. 1970. Axon growth: roles of microfilaments and microtubules. *Proc. Natl. Acad. Sci. USA.* 66:1206–1212.